present study, a family of non-rotating triaxial mass models was used with a central density cusp as observed in the centres of many ellipticals (Crane *et al.,* 1993). These models allow for variations of ellipticity and position angle of major-axis isophotes. They are described in detail by de Zeeuw & Carollo (1996).

Out of the original sample only three galaxies (NGC 1453, NGC 2974 and NGC 7097) turned out to be suitable for modelling. In the remaining objects either presence of several gas components or non-regularities in the velocity field preclude modelling with the gas settled on simple closed orbits. The data of NGC 5077 were also modelled to be compared with the results of Bertola *et al.* (1991). The new model is found to be in reasonable agreement, but better constrained due to the more restrictive geometry (allowing for isophotal twisting). The modelling yielded for NGC 2974 and NGC 7097 that the gas moves on a plane perpendicular to the intrinsic minor axis while in NGC 1453 and NGC 5077 the gas occupies a plane perpendicular to the intrinsic major axis of the galaxy. This would also support the view of the external origin of the gaseous matter.

The resulting mass and light density profiles together with the radial trend of the local M/L_B ratio of NGC 5077 is displayed in Figure 6 as an example for the whole sample. The derived M/L profiles do not show significant radial variations. The M/L ratio seems to be higher for objects of higher optical luminosity. A mean value of $M/L \simeq 5\ M_\odot/L_\odot$ within 1 R_e was derived for the sample. This suggests that the central regions of elliptical galaxies are essentially dominated by luminous matter while dark matter becomes dynamically important only in the range of 2–3 R_e; in this region, however, one has to use the information provided by the stellar kinematics *(e.g.* Saglia *et al.,* 1993; Bertin *et al.,* 1994; Carollo *et al.,* 1995) or resort to other tracers of the gravitational field (Bertola *et al.,* 1993). The use of X-ray data, which extend out to typically $\simeq 7\ R_e$ is not straightforward *(c.f.* Bertin *et al.,* 1993), although a recent combination of ASCA and ROSAT data allowed more precise constraints on the mass distributions for NGC 720 and NGC 1332 (Buote & Canizares, 1997).

The ionised gas proves to be a good tracer of the potential of the host galaxy when compared with stellar kinematical results as in the case of NGC 2974 (Cinzano & van der Marel, 1994).

Acknowledgements

A.P. acknowledges support from a *Acciaierie Beltrame* grant. R.P.S. acknowledges the financial support by the Deutsche Forschungsgemeinschaft under SFB 375. W.W.Z. acknowledges the support of the Hochschuljubiläumstiftung der Stadt Wien (project H-112/95).

References

Baum, S.A. & Heckman, T., 1989, *Astrophys. J.,* **336**, 69.
Bertin, B., Bertola, F., Buson, L.M., Danziger, I.J., Dejonghe, H., Sadler, E.M., Saglia, R.P., Vietri, M., de Zeeuw, P.T. & Zeilinger, W.W.:, 1989, *The Messenger,* **56**,19.
Bertin, G., Bertola, F., Buson, L.M., Danziger, I.J., Dejonghe, H., Sadler, E.M., Saglia, R.P., de Zeeuw, P.T. & Zeilinger, W.W., 1994, *Astron. Astroph., **292**,* 381.
Bertin, G., Pignatelli, E. & Saglia, R.P., 1993, *Astron. Astroph.,* **271**, 381.
Bertola, F. 1992 in *"Morphological and Physical Classification of Galaxies"* ed. Longo, G. et *al., p.* 115.
Bertola, F., Bettoni, D., Danziger, I.J., Sadler, E.M., Sparke, L.S. & de Zeeuw, 1991, *Astrophys. J.,* **373**, 369.
Bertola, F., Pizzella, A., Persic, M. & Salucci, P., 1993, *Astrophys. J.,* **416**, L45.
Bertola, F., Cinzano, P., Corsini, E.M., Rix, H.W. & Zeilinger, W.W., 1995, *Astrophys. J.,* **448**, L13.
Bregman, J.N., Hogg, D.E. & Roberts, M.S., 1992, *Astrophys. J.,* **387**, 484.
Buote, D.A. & Canizares, C.R., 1997, *Astrophys. J.,* in press.
Buson, L.M., Sadler, E.M., Zeilinger, W.W., Bertin, G., Bertola, F., Danziger, I.J., Dejonghe, H., Saglia, R.P. & de Zeeuw, P.T., 1993, *Astron. Astroph.,* **280**, 409.
Caldwell, N., Kirshner, R.P. & Richstone, D.O., 1986, *Astrophys. J.,* **305**, 136.
Carollo, C.M., de Zeeuw, P.T., van der Marel, R.P., Danziger, I.J. & Qian, E.E., 1995, *Astrophys. J.,* **441**, L25.
Cinzano, P. & van der Marel, R.P., 1994, *Mon. Not. R. astr. Soc.,* **270**, 325.
Crane, P. *et al.* 1993, *Astron. J.,* **106**, 1371.
Christodoulou, D.M., Katz, N., Rix, H.W. & Habe, A., 1992, *Astrophys. J.,* **395**, 113.
Demoulin-Ulrich, M.H., Butcher, H.R. & Boksenberg, A., 1984, *Astrophys. J.,* **285**, 527.
Faber, S.M. & Gallagher, J.S, 1976, *Astrophys. J.,* **204**, 365.
Forbes, D.A., 1991, *Mon. Not. R. astr. Soc.,* **249**, 779.
Katz, N. & Rix, H.W., 1992, *Astrophys. J.,* **389**, L55.
Kennicutt, R.C., 1989, *Astrophys. J.,* **344**, 685.
Isnapp, G.R., Turner, E.C. & Cunniffe, P.E., 1985, *Astron. J., **90**,* 454.
Knapp, G.R., Guhathakurta, P., Kim, D.-W. & Jura, M., 1989, *Astrophys. J. Suppl.,* **70**, 387.
Lees, J.F., Knapp, G.R., Rupen, M.P. & Phillips, T.G., 1991, *Astrophys. J.,* **379**, 177.
Macchetto, F. & Sparks, W.B., 1992 in *"Morphological and Physical Classification of Galaxies"* ed. Longo, G. *et al., p.* 191.
Macchetto, F., Pastoriza, M., Caon, N., Sparks, W.B., Giavalisco, M., Bender, R. & Capaccioli, M., 1996 *Astron. Astroph.,* in press.
Phillips, M.M., Jenkins, C.R., Dopita, M.A., Sadler, E.M. & Binette, L., 1986, *Astron. J., **91**,* 1062.
Pizzella, A., Amico, P., Bertola, F., Buson, L.M., Danziger, I.J., Dejonghe, H., Sadler, E.M., Saglia, R.P, de Zeeuw, P.T. & Zeilinger, W.W., 1996 *Astron. Astroph.,* submitted.
Roberts, M.S., Hogg, D.E., Bregman, J.N., Forman, W.R. & Jones, C., 1991, *Astrophys. J. Suppl.,* **75**, 751.
Saglia, R.P., Bertin, B., Bertola, F., Danziger, I.J., Dejonghe, H., Sadler, E.M., Stiavelli, M., de Zeeuw, P.T. & Zeilinger, W.W., 1993, *Astrophys. J., **403**,* 567.
Schweizer, F., 1983, IAU Symp. **100**, p. 319.
Thomas, P.A., Fabian, A.C., Arnaud, K.A., Forman, W. & Jones ,C., 1986, *Mon. Not. R. astr. ,Soc.,* **222**, 655.
Wevers, B.M.R.H. 1984, Ph.D. diss., University of Groningen.
White, III, S. & Sarazin, C.L., 1991, *Astrophys. J.,* **367**, 476.
de Zeeuw, P.T. & Carollo, C.M., 1996, *Mon. Not. R. astr. Soc.,* in press.
Zeilinger, W.W., Pizzella, A., Amico, P., Bertin, G., Bertola, F., Buson, L.M., Danziger, I.J., Dejonghe, H., Sadler, E.M., Saglia, R.P. & de Zeeuw, P.T., 1996, *Astron. Astroph., in* press .

Werner Zeilinger
e-mail: wzeil@doradus.ast.univie.ac.at

The Challenging Type Ia SN 1991bg in the Virgo Galaxy NGC 4374

M. TURATTO [1,2], S. BENETTI [1], E. CAPPELLARO [2], I.J. DANZIGER [1,3], P.A. MAZZALI [3]

[1]European Southern Observatory;
[2]Osservatorio Astronomico di Padova; [3]Osservatorio Astronomico di Trieste, Italy

The long-standing effort in studying type Ia Supernovae (SN Ia) has been motivated in part by their use as distance indicators. Several publications have recently been devoted to the absolute calibration of SN Ia up to the distance of the Virgo cluster using the Cepheids discovered by HST in the SN parent galaxies. It is now commonly believed that the average absolute magnitude of SN Ia at maximum is close to M_B= –19.5, while the average intrinsic colour is $(B - V) \simeq 0.0$ (Tammann et al., 1996).

Nevertheless, it is also recognised that SN Ia are not strictly identical: most SN Ia exhibit a small scatter both in absolute magnitudes and colours. Given the accuracy of modern observations, this scatter cannot be attributed to photometric errors (Patat et al., 1996). This scatter reduces the reliability of SN Ia as standard candles unless a relation is found between the luminosity and some other observational parameter. Indeed, Phillips (1993) and Hamuy et al. (1995) have found a linear relation between the absolute magnitude, M_B, and the rate of decline in the first 15 days past maximum, $\delta(m)_{15}$. Most SNe with $\Delta(m)_{15}$ in the range $1.1 < \Delta(m)_{15} < 1.8$, conform to this relation, but there are exceptions, e.g. SN 1994D (Patat et al., 1996).

Another serious problem has been posed by the discovery of a few SN Ia showing large deviations from the average behaviour. The most extreme among these objects is SN 1991bg in NGC 4374. A spectrum of this SN taken soon after discovery (Benetti et al., 1991) showed most of the typical features of SN Ia, but also some distinct peculiarities. The unusual characteristics motivated the inclusion of this SN among the high priority targets of the ESO Key Programme on SNe. Using five different telescopes (including also the Asiago Observatory 1.8-m) we obtained spectra on 20 nights and photometric measurements on 28 epochs, spanning the period from discovery to eighteen months later.

Whereas a detailed discussion of the results of this remarkable observational effort will appear in two forthcoming papers (Turatto et al., 1996, Mazzali et al., 1996), here we emphasise the most interesting conclusions.

The first striking peculiarity of SN 1991bg is its faint luminosity: the apparent magnitude at maximum was B_{max} = 14.75, about 2.5 mag fainter than that of the two other SN Ia discovered in the same galaxy, SN 1957B and 1980I. In addition, the colour was very red: $(B - V)_{max} = 0.74$ instead of the typical value $(B - V)_{max} = 0.0$. In principle the faint magnitude and the red colour could indicate the presence of strong reddening in the parent galaxy, but this is not expected, since NGC 4374 is an elliptical galaxy. In the spectra, at about 5890Å only a weak interstellar absorption is present. This can be attributed to NaI D within the Galaxy and is consistent with the small galactic extinction in the direction of NGC 4374. Adopting the distance modulus to NGC 4374 obtained with the Surface Brightness Fluctuation method ($\mu = 31.09 \pm 0.30$, Ciardullo et al., 1993), and accounting for a galactic reddening of E(B-V) $\sim 0.05 \pm 0.02$, we obtain for SN 1991bg an absolute magnitude $M_B = -16.54 \pm 0.32$. Even if one assumes for NGC 4374 the Cepheid distance to NGC 4639, which is considered to be located on the far side of the Virgo cluster (25 Mpc, Tammann et al., 1996), SN 1991bg remains 2 mag fainter than the average value for SN Ia.

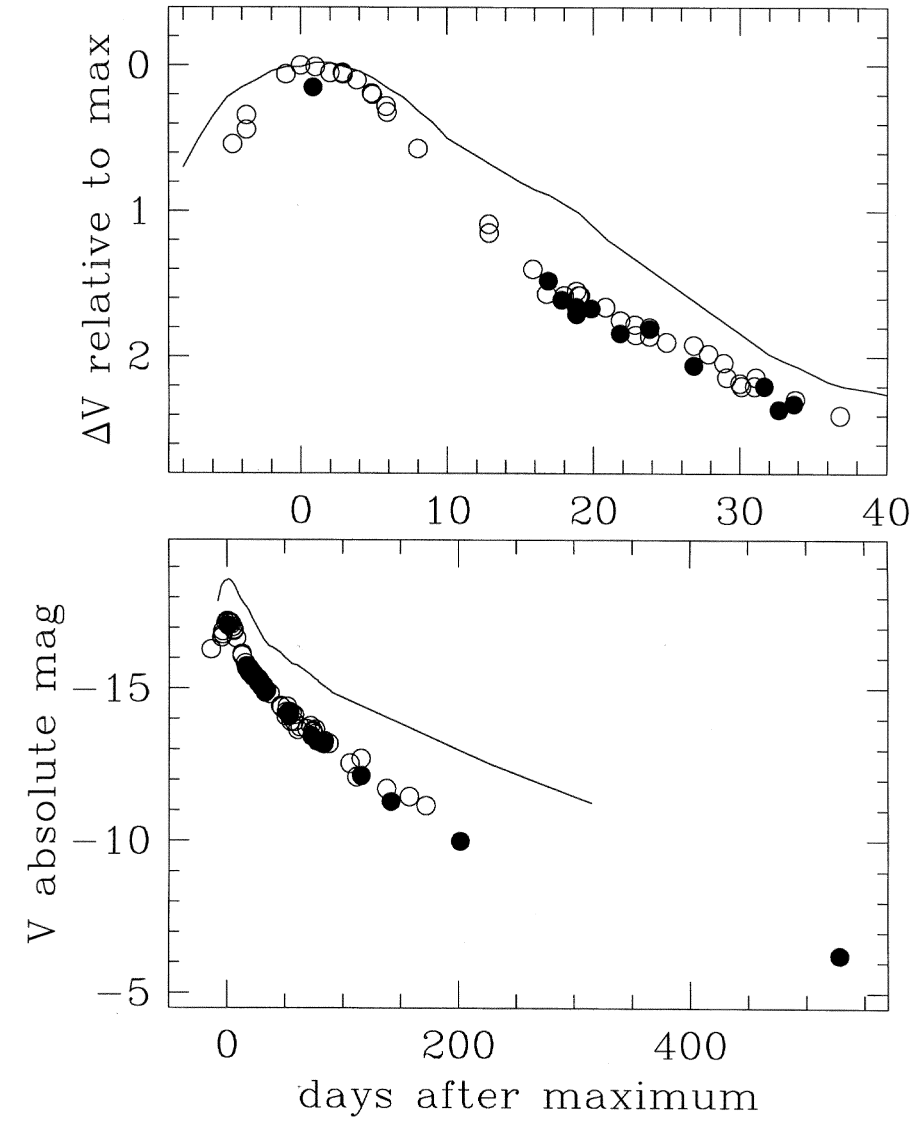

Figure 1: Comparison of the V light curve of SN 1991bg with that of the normal SN Ia 1992A. In the upper panel, the fast luminosity evolution of SN1991bg near maximum light is emphasised. In the lower panel, the comparison of the absolute magnitudes shows that SN 1991bg was about three times fainter at maximum and, because of the more rapid evolution, the difference increases to a factor 5 on day 200. Filled symbols are our measurements and open symbols are measurements from Filippenko et al. (1992) and Leibundgut et al. (1993). At early epochs the agreement between the different sources is good, but it becomes poor as the SN fades. Since the zero point is the same (the local sequences coincide), the inconsistency is attributed to the measuring technique. We measured the magnitudes using the point spread function fitting with Romafot and with Snoopy, a package for SN photometry developed by F. Patat.

Additional photometric peculiarities are the very narrow light curve and the steep luminosity decline, $\beta_B = 14.7$ *mag* $\times (100d)^{-1}$, to be compared with a typical value $\beta_B = 12$ *mag* $\times (100d)^{-1}$ as measured for SN 1992A (Fig. 1). Moreover, the I light curve shows no sign of the secondary maximum which is normally seen in other SN Ia about 3 weeks after the primary one. The rapid evolution is indicative of a small mass of the ejecta. In fact, a small mass implies a less efficient trapping of the γ-rays from the radioactive decays and a more rapid decrease of temperature than in "normal" SN Ia. As a consequence, the photosphere recedes faster in mass co-ordinates, and a steep luminosity decline is observed.

Owing to the extensive coverage in several photometric bands, it was possible to obtain the *uvoir* bolometric luminosity for SN 1991bg. At maximum, this was log L = 42.20 erg s^{-1}, i.e. about 3 times fainter than the "normal" SN Ia SN 1992A (log L = 42.65, Suntzeff, 1996). In the scenario where the SN light curve is powered by the radioactive decay of ^{56}Ni–^{56}Co–^{56}Fe, there is a direct relationship between the luminosity at maximum and the amount of ^{56}Ni produced in the explosion, although the actual estimate of the mass of radioactive material may vary by as much as 50% depending

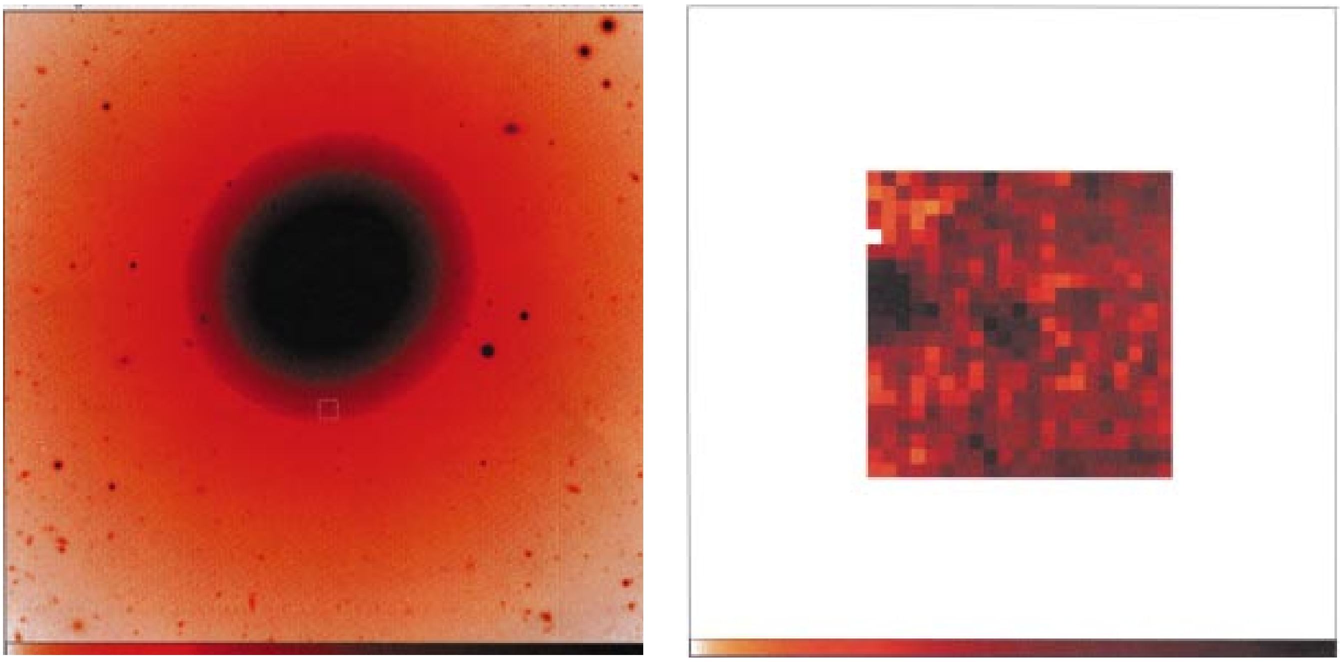

Figure 2: Co-added V image of NGC 4374 (left) obtained on May 26, 1993 (i.e. 530 days after maximum) at the NTT (+EMMI) (total exposure 170 min.). The location of SN 1991bg is marked. The SN region is enlarged and background subtracted on the right panel. Though the seeing was not exceptional (~ 1.15 arcsec), the SN was detected at V = 24.95 ± 0.40.

on the explosion mechanism. If we adopt the so-called “standard model”, where normal SN Ia produce about 0.6 $M_{\odot}$ of Ni, then SN 1991bg produced only about 0.2 $M_{\odot}$.

Theoretical models of both early- and late-time spectra suggest that not only the Ni mass is small ($\sim 0.1 M_{\odot}$), but that the ejected mass was also small: ~ 0.6 $M_{\odot}$ compared to 1.4 $M_{\odot}$ for “normal” SN Ia. Assuming that no remnant was left over, this indicates that SN 1991bg was the result of the explosion of a sub-Chandrasekhar mass progenitor.

Focusing on the spectra, SN 1991bg shows most of the typical SN Ia features due to intermediate-mass elements, in particular the strong SiII λ6355 absorption, although with noticeable differences in the relative line intensities. The most distinctive peculiarities are the presence of an absorption between 4200 and 4500Å, attributed to TiII, and the low expansion velocity of the photosphere, v_{max} = 9700 km s^{-1} instead of about v_{max} = 12,000 km s^{-1} measured for SN 1992A.

The fast photometric evolution of SN 1991bg has its spectral counterpart in the early appearance of the nebular lines. Already on day 34 a relatively narrow emission line appeared at a rest frame wavelength of about 5900Å. Because of the close coincidence in wavelength, the line was identified with the NaID line, but in the light of the spectral modelling of Mazzali et al. (1996) we propose a significant contribution from [CoIII] λ5890–5908.

The ESO observations are especially interesting for the description of the late-time behaviour of SN 1991bg. Even at late epochs the fading rate continues to be significantly faster than those of all other well-observed SN Ia. For instance in the V band the luminosity decline rate between 70 and 200 days was 2.7 *mag* $\times (100d)^{-1}$ while typical rates for SN Ia are about 1.5 *mag* $\times (100d)^{-1}$. With the observation shown in Figure 2 we were able to detect the SN 530 days after maximum. This last point indicates that luminosity decline slowed down significantly and became consistent, within the errors, with the radioactive decay of ^{56}Co to ^{56}Fe (0.98 mag $\times$ (100d)$^{-1}$). Assuming for day 530 the same spectral distribution as on day 203, the corresponding *vvoir* bolometric luminosity was log $L \sim 38.0$ ergs s^{-1}.

The latest spectral observation of SN 1991bg was secured 203 days after maximum. This is compared in Figure 3 with SN 1992A at a similar epoch. Contrary to previous claims, the same features are present in both spectra, although they are definitely narrower in SN 1991bg. The narrow width of the lines makes the identification of the related atomic transition easier than in normal SN Ia. The identifications are shown in Figure 3 and are based on the modelling presented in Mazzali et al. (1996). All lines find satisfactory identifications with forbidden lines of Fe-group elements, with one exception. In previous work this line was measured at 6570 Å in the galaxy rest frame and hence identified with Hα. Actually the correct wavelength (obtained averaging the positions measured in three spectra) is 6590 ± 5 Å. Although we cannot rule out the possibility of high-velocity blobs emitting redshifted hydrogen lines, according to our spectral modelling we suggest the identification with [CoIII] λ6578 as a possibility.

All observations indicate a scenario in which an under-energetic explosion took place in a low-mass progenitor. The weaker explosion provided less kinetic energy and a smaller amount of radioactive ^{56}Ni which in turn provided less energy to the light curve than in most SN Ia.

The existence of this unusually faint SN Ia immediately raises the question how many of these explosions occur. So far, few other SN Ia with some of the characteristics of SN 1991bg have been observed, namely SNe 1986G, 1991F and 1992K, but none of them as extreme as SN 1991bg. On the other hand, it is known that overluminous SN Ia also exist, the best example being SN 1991T (cf. Ruiz-Lapuente et al., 1992, Phillips et al., 1992, Mazzali et al., 1995).

In the context of the use of SN Ia as distance indicators, one should take care to use only those SNe which did not show photometric or spectroscopic peculiarities. Hence one should use only those SNe for which good signal-to-noise observations and an adequate temporal and spectral coverage are available.

However, when detailed modelling will be available for a good sample of SNe, it might became possible to establish diagnostic criteria correlating spectral properties and luminosity. At that point, thanks to an individual spectrophotometric calibration there may be no “peculiar” objects, but only a sequence of SNe, all of them useful as distance indicators. Some early results in this direction have already been obtained (e.g. Hoflich & Khokhlov, 1995) but much still has to be done from both the observational and the theoretical point of view.

References

[1] Benetti, S., Cappellaro, E., Turatto, M., 1991, IAUC 5405.

[2] Ciardullo, R., Jacoby, G.H., Tonry, J.L., 1993, *ApJ* **419**, 479.

[3] Filippenko, A.V., Richmond, M.W., Branch, D., Gaskel, C.M., Herbst, W., Ford, C.H., Treffers, R.R., Matheson, T., Ho, L.C., Dey, A., Sargent, W.L.W., Small, T.A., Bruegel, W.J.M., 1992, *AJ* **104**, 1543..

[4] Hamuy, M., Phillips, M.M., Maza, J., Suntzeff, N.B., Schommer, R.A., Aviles, R., 1995, *AJ* **109**, 1.

[5] Hoflich, P., Khokhlov, A.M., 1995, *ApJ* **457**, 500.

[6] Leibundgut, B., Kirshner, R., Phillips, M.M., et al., 1993, *AJ* **105**, 301.

[7] Mazzali P.A., Chugai, N., Turatto, M., Lucy, L., Danziger, I.J., Cappellaro, E., Della Valle, M., Benetti, S., 1996, *MNRAS* in press.

[8] Mazzali P.A., Danziger, I.J., Turatto, M., 1995, *A&A* **297**, 509.

[9] Patat, F., Benetti, S., Cappellaro, E., Danziger, I.J., Della Valle, M., Mazzali, P., Turatto, M., 1996, *MNRAS* **278**, 111.

[10] Phillips, M.M., 1993, *ApJ* **413**, L105.

[11] Phillips, M.M., Wells, L.A., Suntzeff, N.B., Hamuy, M., Leibundgut, B., Kirshner, R.P., Foltz, C.B., 1992, *AJ* **103**, 1632.

[12] Ruiz-Lapuente, P., Cappellaro, E., Turatto, M., Gouiffes, C., Danziger, I.J., Della Valle, M., Lucy, L.B., 1992, *ApJ* **387**, L33.

[13] Suntzeff, N.B., 1996, in *Supernova and Supernova Remnants*, McCray, R. & Wang, Z., ed., Cambridge University Press, Cambridge, p.41.

[14] Tammann, G.A., Labhardt, L., Federspiel, M., Sandage, A., Saha, A., Macchetto, F.D., Panagia, N., 1996, in *Science with the Hubble Space Telescope II*, eds. Benvenuti, P., Macchetto, F.D. & Schreier, E.J., STScI/ST-ECF Workshop, p. 9.

[15] Turatto, M., Benetti, S., Cappellaro, E., Danziger, I.J., Della Valle, M., GouiffeS, C., Mazzali, P., Patat, F., 1996, *MNRAS* in press.

Massimo Turatto
e-mail: mturatto@eso.org

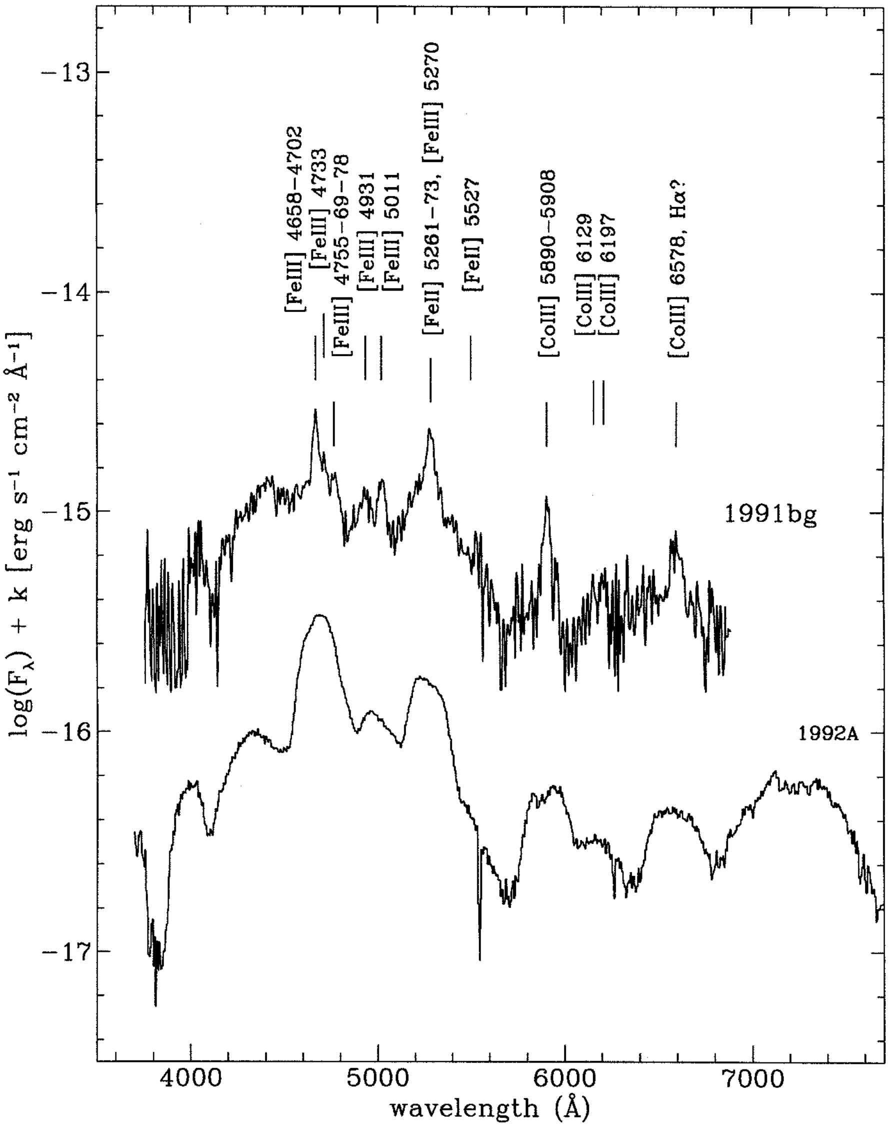

Figure 3: Comparison of the late spectra of SNe 1991bg (203 days) and 1992A (227 days), both obtained with EFOSC1 at the 3.6-m telescope. The identifications of the main emission lines are based on the NLTE models by Mazzali et al. (1996).

Long-Slit Echelle Spectroscopy at the NTT

R.L.M. CORRADI[1], A. MAMPASO[1], M. PERINOTTO[2]

[1]Instituto de Astrofísica de Canarias, Tenerife, Spain

[2]Dipartimento di Astronomia e Scienza dello Spazio, Università di Firenze, Italy

During our recent observing run at La Silla (April 26–28, 1996), we had the chance to experiment successfully a previously unexplored capability of the NTT: high-dispersion spectroscopy using the full slit length of EMMI.

The EMMI-REMD (REd Medium Dispersion) spectroscopic mode is provided with three echelle gratings (#9, #10, and #14), which give spectral resolving powers of 7700, 28,000, and 60,000, respectively, for a slit width of 1″ and the actual Tek 2048 × 2048 CCD #36. These gratings are normally coupled to a grism which acts as a cross-disperser to obtain conventional multi-order echelle spectroscopy. The closeness of adjacent orders, while providing a large total spectral coverage, limits the usable slit length to a few arcseconds. For several astrophysical applications, however, it would be highly desirable to have a longer slit. This can be obtained by taking off the cross-disperser, and isolating one echelle order by means of a narrow-band filter mounted in the filter wheel unit (see the *ESO Operating Manual* No. 15, Zijlstra et al., 1996, for more details). In this way, one can take advantage of the full length of the EMMI-REMD slit (6 arcmin!), and work at very high spectral and spatial resolutions (R ≤ 70000, with a spatial scale of 0.27″ pix^{-1}, matching excellent seeing conditions which are not infrequent at the NTT).

With this configuration, the spectral coverage is of course limited to few manometers by the width of the narrow-band filter, and normally includes one or few spectral features. It is, however, a very powerful combination for many applications which concern the observation of extended objects with narrow spectral features, such as Galactic HII nebulae, and possibly external galaxies.